SUPPORTING INFORMATION

Framework and Extraframework Tin Sites in Zeolite Beta React Glucose Differently

Ricardo Bermejo-Deval[†], Rajamani Gounder[†] and Mark E. Davis*

Chemical Engineering, California Institute of Technology, Pasadena, California 91125, United States

*Corresponding author. E-mail: mdavis@cheme.caltech.edu

[†]R.B.D. and R.G. contributed equally to this work.

S.1. X-ray diffractograms of zeolite samples.

Powder x-ray diffraction patterns of the samples in this study are shown in Figure S.1.

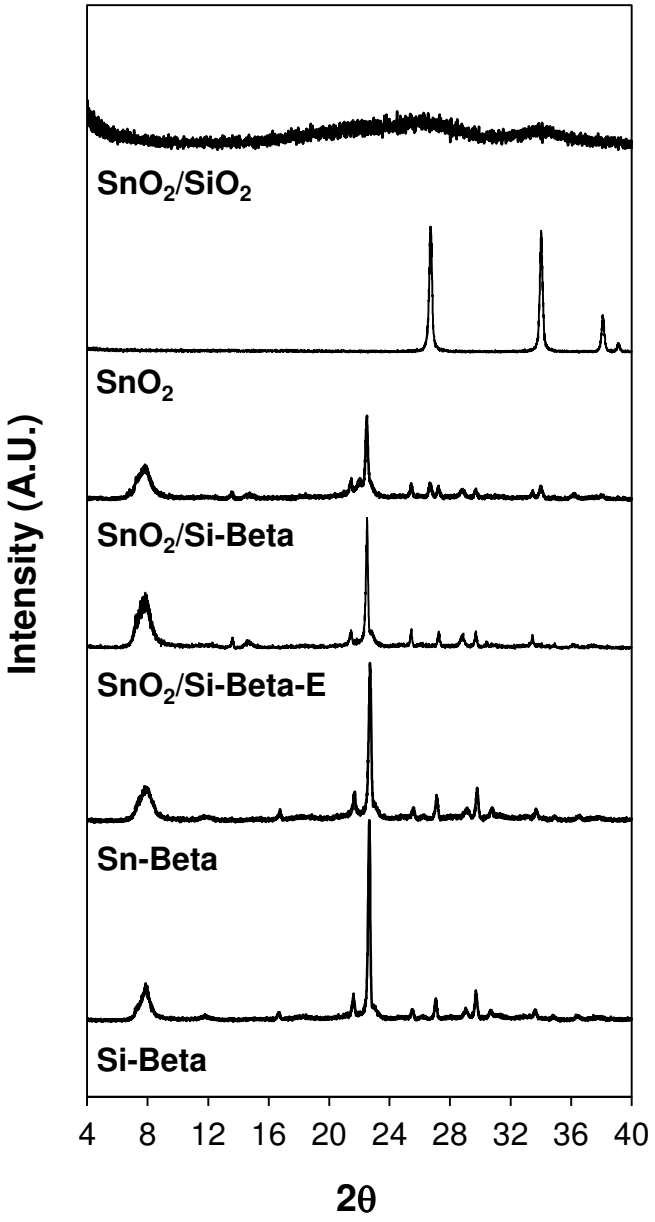

Figure S.1. Powder x-ray diffraction patterns of Si-Beta, Sn-Beta, SnO_2/Si-Beta-E, SnO_2/Si-Beta, SnO_2, SnO_2/SiO_2 (bottom to top).

S.2. SEM images of zeolite samples.

SEM images of Sn-Beta and SnO_2/Si-Beta are shown at different magnifications in Figure S.2.

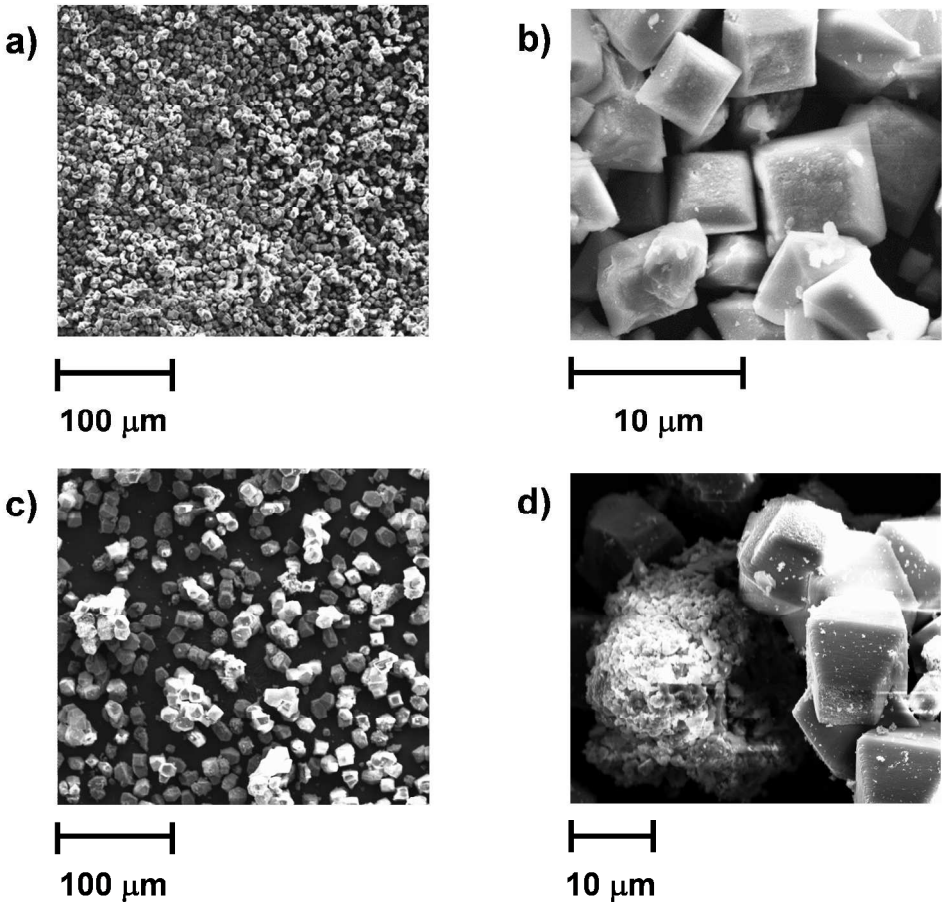

Figure S.2. SEM images of (a, b) Sn-Beta and (c, d) SnO_2/Si-Beta.

S.3. N_2 adsorption isotherms of zeolite samples.

N_2 adsorption isotherms (77 K) are shown for Si-Beta (Fig. S.3), Sn-Beta (Fig. S.4), SnO_2/Si-Beta-E (Fig. S.5) and SnO_2/Si-Beta (Fig. S.6). Total micropore volumes were determined from linear extrapolation of N_2 uptakes in mesopore regions (P/P_0 ~ 0.1-0.4) to zero relative pressure and from the liquid N_2 molar density (0.029 mol cm^{-3}). This method gave values of 0.19, 0.20, 0.20 and 0.12 cm^3 g^{-1} for Si-Beta, Sn-Beta, SnO_2/Si-Beta-E and SnO_2/Si-Beta, respectively. The value for SnO_2/Si-Beta (0.12 cm^3 g^{-1}) is lower than expected if SnO_2 domains (2.67 wt%, 6.95 g cm^{-3}) were located in extracrystalline phases of Si-Beta (0.185 cm^3 g^{-1}) or occluded volume within Si-Beta voids (0.181 cm^3 g^{-1}), suggesting that SnO_2 particles within the pores of SnO_2/Si-Beta also prevent access to a fraction of the intracrystalline void volume.

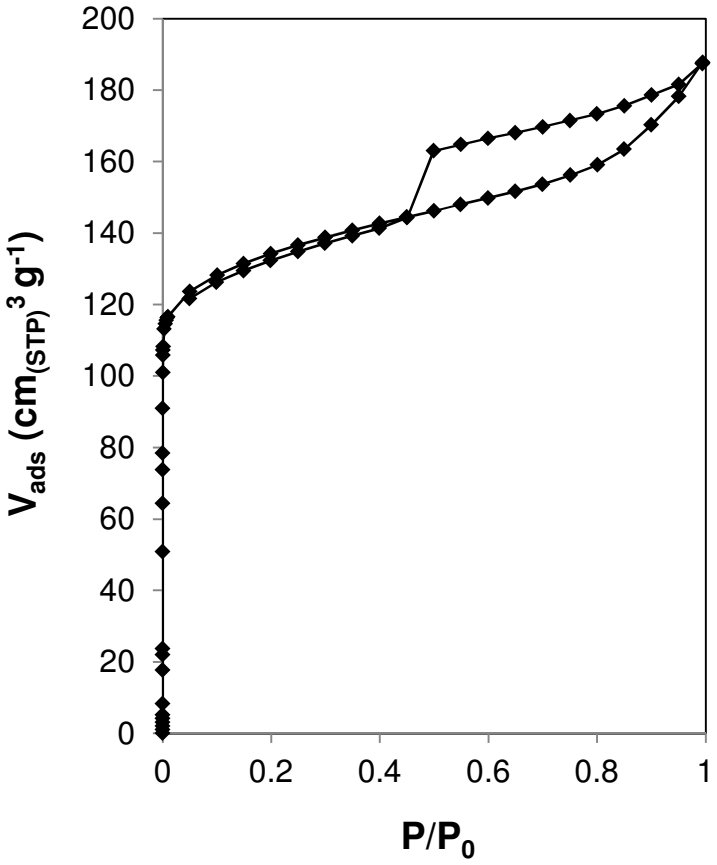

Figure S.3. N_2 adsorption isotherm (77 K) for Si-Beta.

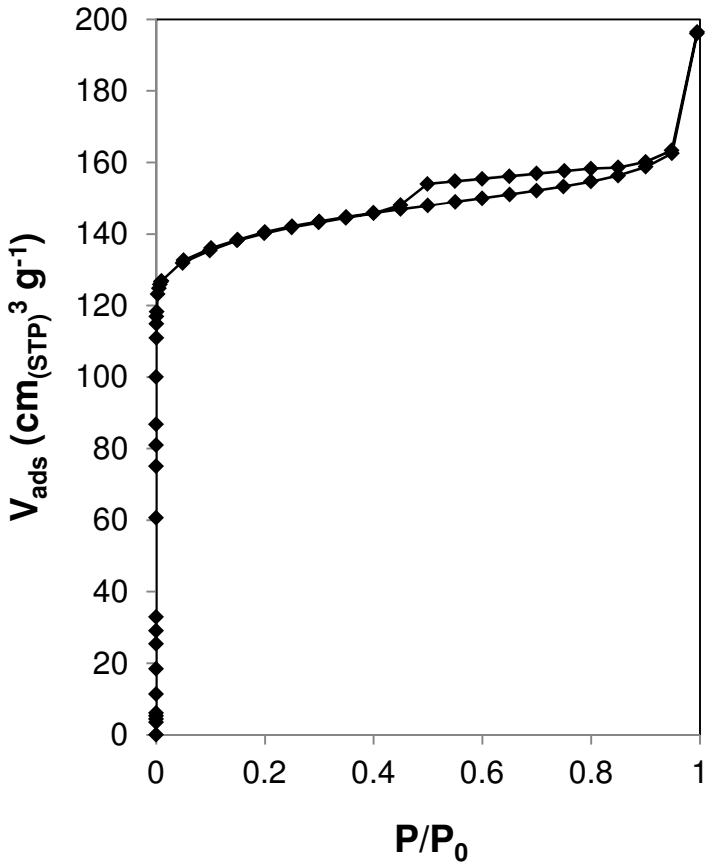

Figure S.4. N_2 adsorption isotherm (77 K) for Sn-Beta.

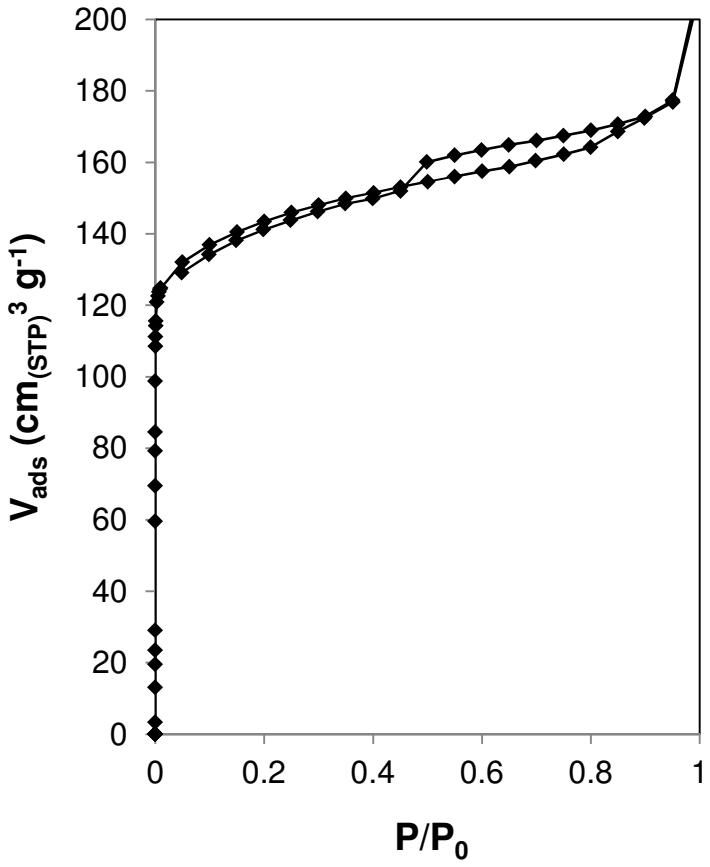

Figure S.5. N_2 adsorption isotherm (77 K) for SnO_2/Si-Beta-E.

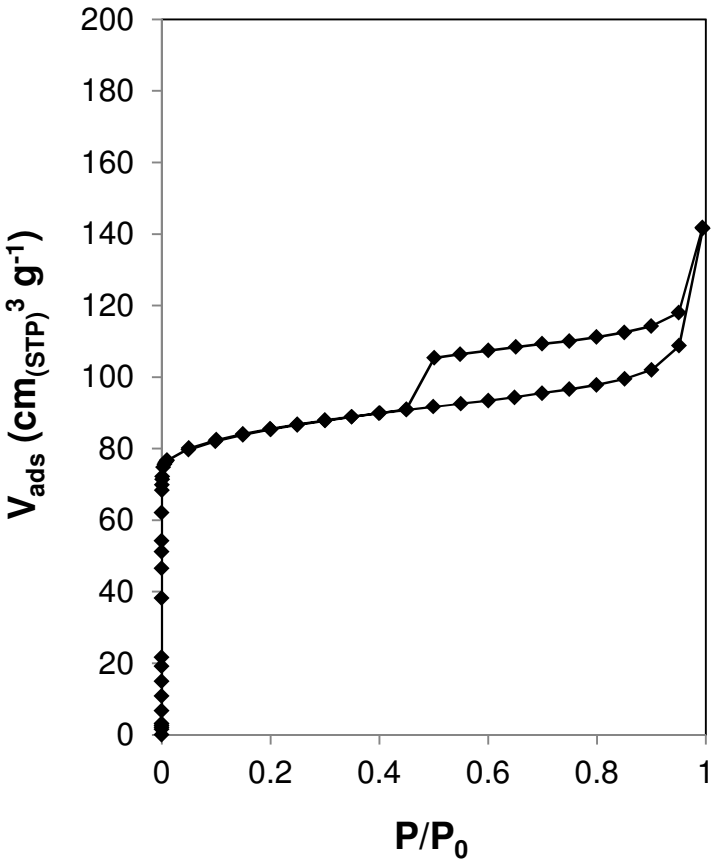

Figure S.6. N_2 adsorption isotherm (77 K) for SnO_2/Si-Beta.

S.4. Turnover rates for glucose isomerization and epimerization.

Turnover rates for glucose isomerization to fructose (Sn-Beta in H_2O, SnO_2/Si-Beta in H_2O and CH_3OH, and SnO_2/SiO_2 in CH_3OH) and epimerization to mannose (Sn-Beta in CH_3OH) as a function of temperature are given in Table S.1. These data are plotted in Figures 1 and 2 of the main text and in Figure S.10 of the supporting information.

Table S.1. Turnover rates for glucose conversion on Sn-Beta, SnO_2/Si-Beta and SnO_2/SiO_2 in H_2O and CH_3OH solvents.

Catalyst	**Solvent**	**Turnover rate** ($/ 10^{-3}$ mol s^{-1} (mol Sn)$^{-1}$)					
		333 K	***343 K***	***353 K***	***363 K***	***373 K***	***383 K***
Sn-Beta	H_2O	-	2.5 ± 1.9	3.8 ± 1.2	16.4 ± 6.1	27.8 ± 5.0	-
	CH_3OH	-	1.0 ± 0.3	2.0 ± 0.4	3.8 ± 1.0	7.4 ± 1.4	13.3 ± 3.1
SnO_2/Si-Beta	H_2O	1.3 ± 0.2	2.0 ± 0.3	3.5 ± 0.3	4.8 ± 0.7	9.7 ± 1.9	20.7 ± 2.7
	CH_3OH	1.8 ± 0.2	3.6 ± 0.9	9.2 ± 2.1	14.1 ± 3.2	16.6 ± 2.3	19.2 ± 2.9
SnO_2/SiO_2	H_2O	n.d.*	n.d.*	n.d.*	n.d.*	n.d.*	n.d.*
	CH_3OH	-	0.2 ± 0.04	0.7 ± 0.1	2.0 ± 0.3	4.2 ± 0.3	-

*n.d. not detected

S.5. ^{1}H and ^{13}C NMR spectra of sugars after reaction of glucose-D2 with SnO_2/Si-Beta in water.

The ^{1}H NMR spectrum of the glucose fraction after reaction of glucose-D2 with SnO_2/Si-Beta in water is shown in Figure S.7. The resonance near δ = 3.1 ppm reflects the presence of a proton at the C-2 position in glucose. This suggests that D-atoms initially located at the C-2 position have been scrambled isotopically, as expected from the formation of enolate species via SnO_2-catalyzed proton abstraction at the α-carbonyl carbon atom of glucose. We have previously reported the scrambling of D-atoms at the C-2 position when glucose-D2 is isomerized via the proton-transfer mechanism in aqueous NaOH (resonance at δ = 74.1 ppm, Fig. S.8d), but not when isomerized via the intramolecular hydride shift mechanism on Sn-Beta in water (no resonance at δ = 74.1 ppm, Fig. S.8c).

Enolate intermediates can form unlabeled glucose via reprotonation, or unlabeled fructose via isomerization. The resonance δ = 3.45 ppm in the fructose fraction after reaction glucose-D2 with SnO_2/Si-Beta in water (Fig. S.9) confirms the presence of a proton at the C-1 position in fructose. We have previously reported that the deuterium atoms are retained at C-1 positions in fructose when isomerization occurs on Sn-Beta (no resonances at δ = 63.8 and 62.6 ppm, Fig. S.8f), but are not retained when isomerization occurs on aqueous NaOH (resonances at δ = 63.8 and 62.6 ppm, Fig. S.8g).

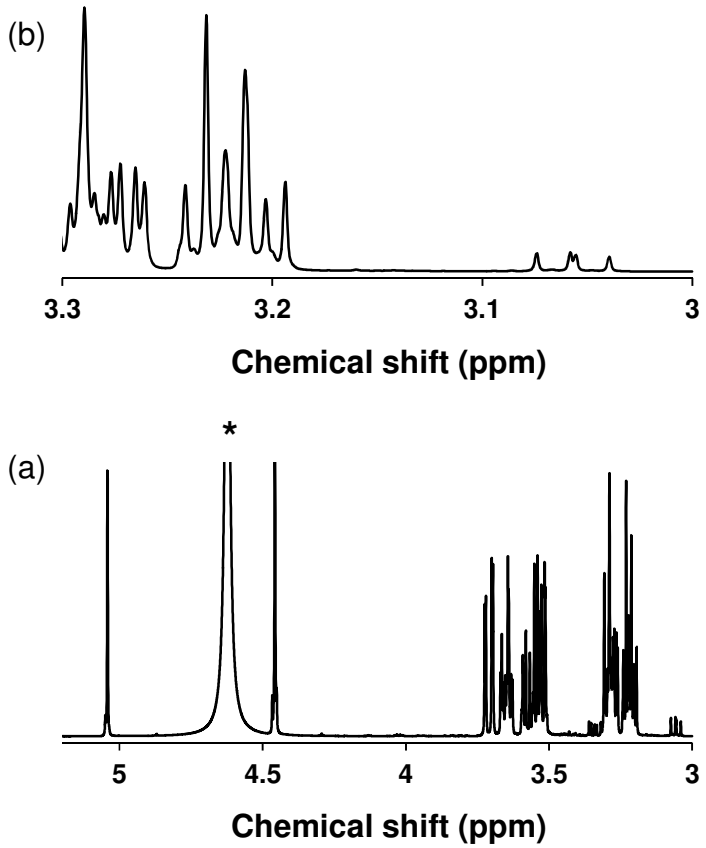

Figure S.7. ^{1}H NMR spectrum of glucose fraction after reaction of glucose-D2 with SnO_2/Si-Beta in water at 373 K for 1h. (a) δ: 3-5.2 ppm; * denotes H_2O. (b) δ: 3-3.3 ppm.

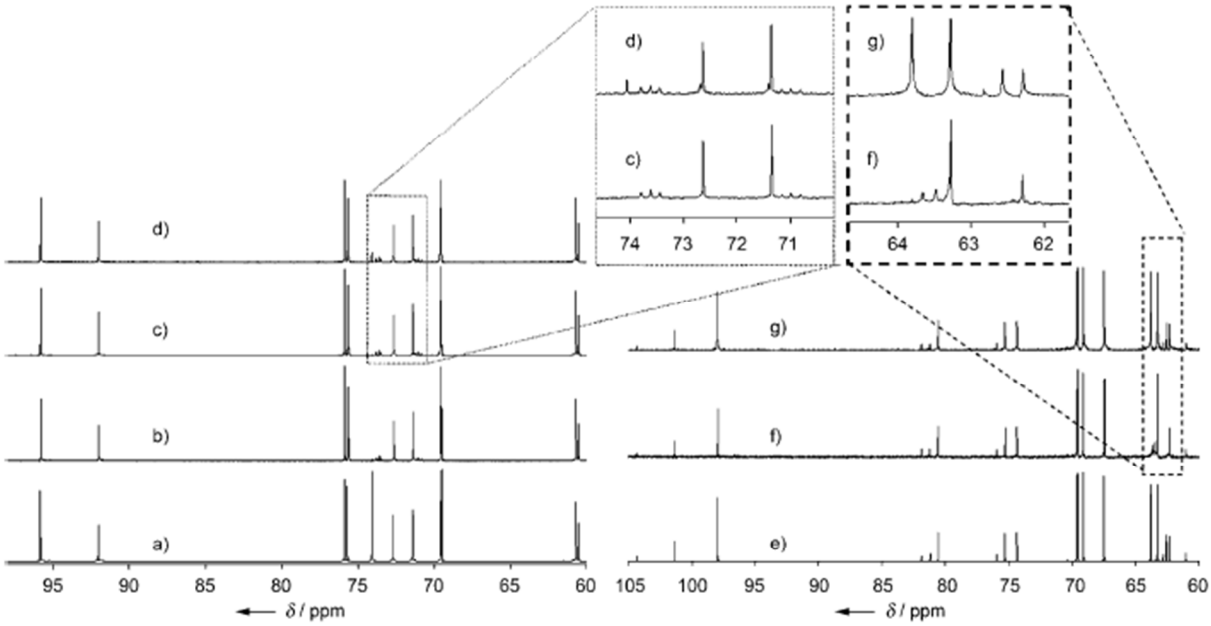

Figure S.8. ^{13}C NMR spectra of a) unlabeled glucose, b) labeled glucose-D2, c) glucose fraction obtained after reacting glucose-D2 with Sn-Beta, d) glucose fraction obtained after reacting labeled glucose-D2 with NaOH, e) unlabeled fructose, f) fructose fraction obtained after reacting labeled glucose-D2 with Sn-Beta, and g) fructose fraction after reacting labeled glucose-D2 with NaOH. Reproduced with permission from reference 3 (Y. Roman-Leshkov, M. Moliner, J. A. Labinger and M. E. Davis, *Angew. Chem.-Int. Edit.*, 2010, **49**, 8954-8957), copyright 2010, Wiley-VCH Verlag GmbH & Co. KGaA, Weinheim.

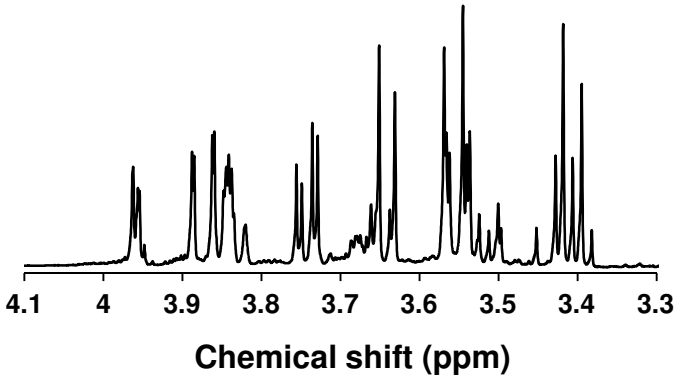

Figure S.9. ^{1}H NMR spectrum of fructose fraction after reaction of glucose-D2 with SnO_2/Si-Beta in water at 373 K for 1 h.

S.6. Apparent activation energies for glucose isomerization on SnO_2/Si-Beta and SnO_2/SiO_2 in methanol

Turnover rates of glucose isomerization to fructose in methanol solvents on SnO_2 domains confined within micropores of zeolite beta (SnO_2/Si-Beta) and dispersed on amorphous silica (SnO_2/SiO_2) are shown in Figure S.10 as a function of temperature. On SnO_2/SiO_2 in methanol, for which diffusion of reactants to SnO_2 surfaces are not expected to limit rates, the apparent activation energy is 102 $\pm$ 9 kJ mol^{-1}. These values are similar to those measured for glucose isomerization catalyzed homogenously in aqueous alkaline media (~120 kJ mol^{-1}). These data imply that the apparent activation energy should be ~51 kJ mol^{-1} on a catalyst with severe internal mass transfer limitations and for which diffusion is a weakly activated process (E_{app} = 0.5 *E_{true}; Davis, M. E., Davis, R. J. *Fundamentals of Chemical Reaction Engineering*, McGraw-Hill: New York, 2003, pgs. 207-208).

On SnO_2/Si-Beta in methanol, the apparent activation energy between 333-363 K is 71 $\pm$ 15 kJ mol^{-1} and is similar to the value measured on SnO_2/Si-Beta in water (59 $\pm$ 6 kJ mol^{-1}; Table 2). The lower barriers measured on SnO_2/Si-Beta compared to SnO_2/SiO_2 are consistent with the presence of internal diffusional limitations and with non-negligible barriers for glucose diffusion within zeolite Beta micropores compared to barriers for glucose isomerization to fructose. The apparent activation energy for glucose isomerization on SnO_2/Si-Beta in methanol is even lower between 363-383 K (18 $\pm$ 5 kJ mol^{-1}), which may reflect contributions from extracrystalline mass transfer limitations.

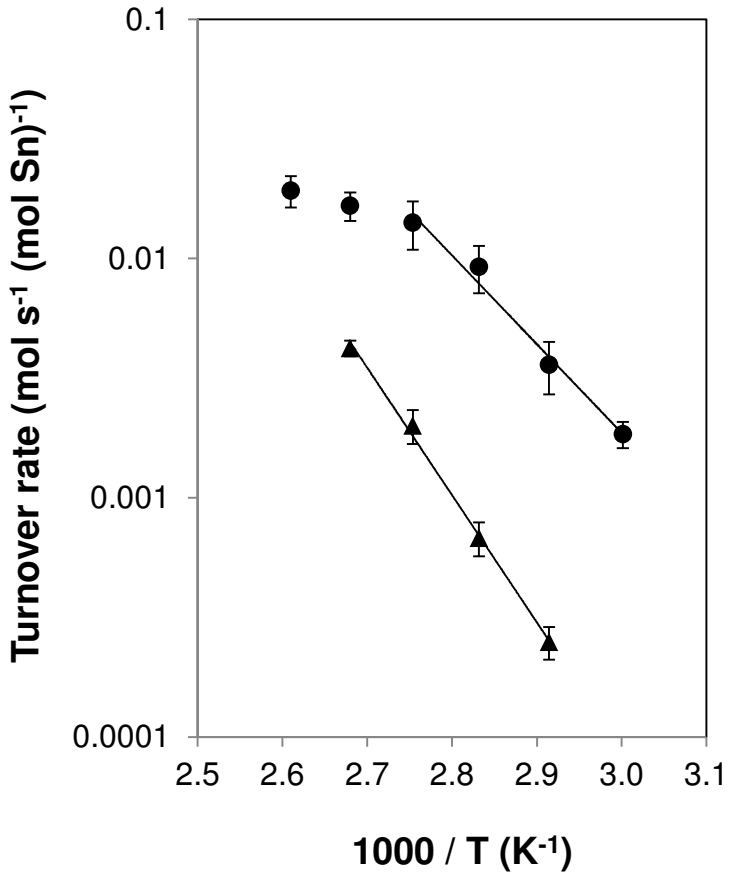

Figure S.10. Temperature dependence of turnover rates for glucose isomerization to fructose in methanol on SnO_2/Si-Beta (circles) and SnO_2-SiO_2 (triangles).

S.7. ^{1}H NMR spectra of sugars after reaction of glucose-D2 with SnO_2/Si-Beta in methanol.

The ^{1}H NMR spectrum of the glucose fraction after reaction of glucose-D2 with SnO_2/Si-Beta in methanol is shown in Figure S.11. The resonance at δ = 3.1 ppm is assigned to a proton at the C-2 position in glucose, indicating isotopic scrambling of some of the D-atoms in glucose. These observations are consistent with the formation of enolate species via SnO_2-catalyzed proton abstraction at the α-carbonyl carbon atom of glucose-D2, which can reprotonate to form unlabeled glucose or isomerize to form unlabeled fructose. The resonance δ = 3.45 ppm in the fructose fraction after reaction glucose-D2 with SnO_2/Si-Beta in methanol (Fig. S.12) confirms the presence of a proton at the C-1 position in fructose, in contrast to the deuterium expected if isomerization were to occur via an intramolecular hydride shift.

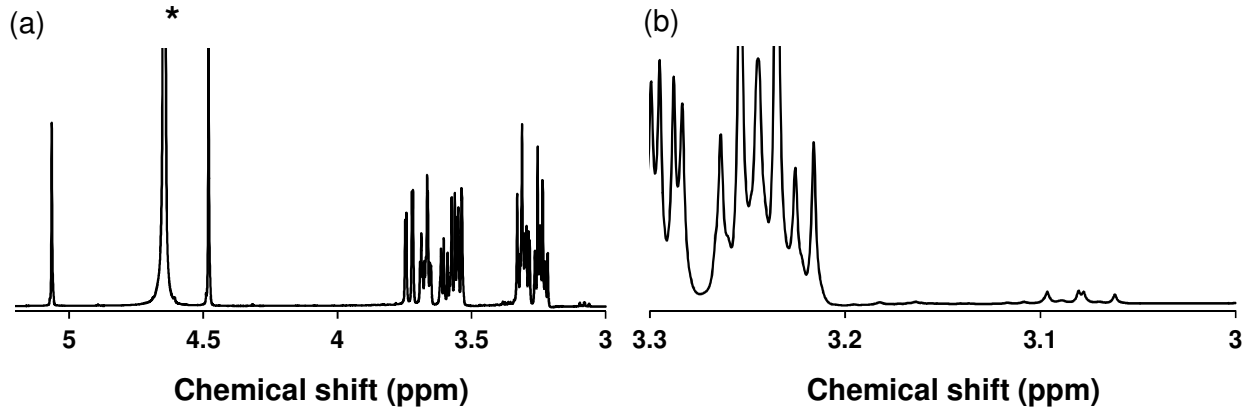

Figure S.11. ^{1}H NMR spectrum of glucose fraction after reaction of glucose-D2 with SnO_2/Si-Beta in methanol at 373 K for 1 h. (a) δ: 3-5.2 ppm; * denotes H_2O. (b) δ: 3-3.3 ppm.

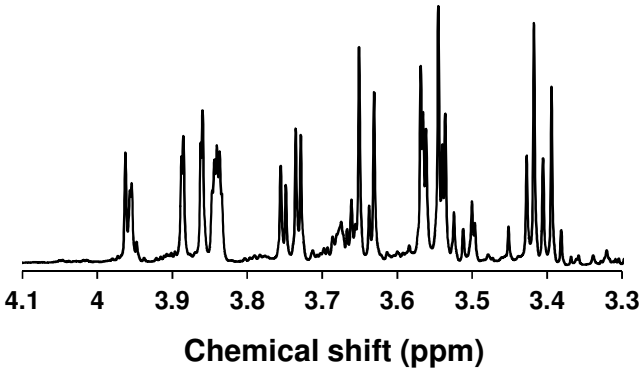

Figure S.12. ^{1}H NMR spectrum of fructose fraction after reaction of glucose-D2 with SnO_2/Si-Beta in methanol at 373 K for 1 h.

S.8. ^{13}C NMR spectra of fructose products formed from reaction of glucose-^{13}C-C1 with Sn-Beta in methanol and water.

The ^{13}C NMR spectrum of the fructose fraction after reaction of glucose-^{13}C-C1 with Sn-Beta in methanol is shown in Figure S.13. Resonances appear for the C-1 position (δ = 63.8 and 62.6 ppm; ~68% of the total area) and C-2 position (δ = 98.0 and 101.4 ppm; ~32% of the total area) of the β-pyranose and β-furanose forms of fructose. These data suggest that fructose is formed from both glucose-^{13}C-C1 and mannose-^{13}C-C2.

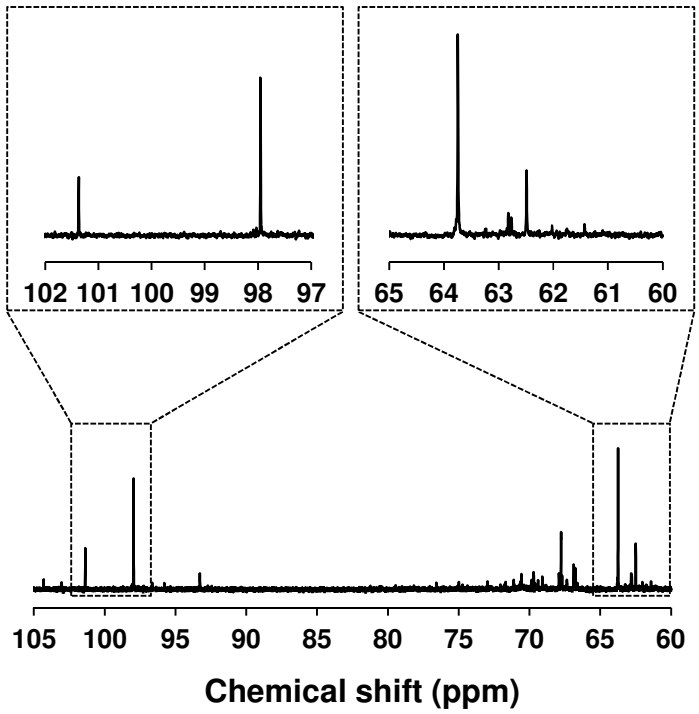

Figure S.13. ^{13}C NMR spectrum of fructose fraction after reaction of glucose-^{13}C-C1with Sn-Beta in methanol at 373 K for 4 h.

The ^{13}C NMR spectrum of the fructose fraction after reaction of glucose-^{13}C-C1 with Sn-Beta in water is shown in Figure S.14. Resonances appear predominantly (~90% of the total area) for the C-1 position (δ = 63.8 and 62.6 ppm) of the β-pyranose and β-furanose forms of fructose. These data are consistent with glucose isomerization to fructose via the hydride-shift mechanism, which does not involve carbon shift along the sugar backbone.

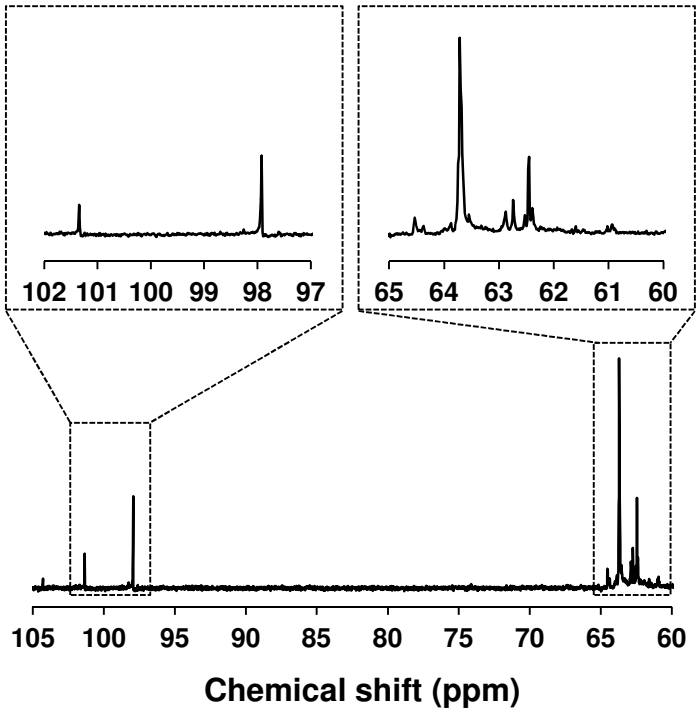

Figure S.14. ^{13}C NMR spectrum of fructose fraction after reaction of glucose-^{13}C-C1with Sn-Beta in water at 373 K for 90 min.